Optical Properties of Antimonene Monolyaers

D. Singh[1], S. K. Gupta[2], Y. Sonvane[1], G. Wang[3], I. Lukacevic[4] and R. Pandey[3,*]

[1]Department of Applied Physics, S. V. National Institute of Technology, Surat, 395007, India.

[2]Department of Physics and Electronics, St. Xavier's College, Ahmedabad, 380009, India.

[3]Department of Physics, Michigan Technological University, Houghton, 49931, USA.

[4]Department of Physics, University J. J. Strossmayer, 31000 Osijek, Croatia.

ABSTRACT

In the present study, we have calculated optical properties of these α and β allotropes of antimonene monolayers. The dielectric matrix has been calculated within the random phase approximation (RPA) using density functional theory. We have calculated dielectric function, absorption coefficient, refractive index, electronic energy loss spectroscopy and optical reflectivity are performed in the energy range 0 to 25 eV. Our calculations show that the β-Sb has more appropriate than α-Sb in the microelectronic, optoelectronics devises and solar cell applications.

(September 10, 2015)

***Email:** pandey@mtu.edu

INTRODUCTION

2D monolayer like well known graphene and other family has lot of scope in future technology to manipulate its optical properties. Very recently, antimonene (Sb), [G. Wang, R. Pandey and S. P. Karna, ACS Appl. Mater. Interfaces, 7, 11490−11496 (2015)] a layered material consisting of sheets of sp^3-hybridized antimony atoms puckered along the so-called in-plane armchair direction and held together by weak van-der Waals forces, has been the focus of a considerable amount of research into its electronic, and structural properties [O. U¨ zengi Aktu¨rk, V. Ongun O¨ zc¸elik, and S. Ciraci, PHYSICAL REVIEW B 91, 235446 (2015)]. It will be interesting to growth of antimonene (Sb) by the isolation of the few-layer forms of antimonene (Sb) for spectroscopic and electrical characterization. Like other ultrathin two-dimensional (2D) crystals [B. Amin, N. Singh, and U. Schwingenschl¨ogl, PHYSICAL REVIEW B 92, 075439 (2015) and Y. Zhao, Y. Zhang, Z. Yang, Y. Yan, and K. Sun, Sci. Technol.Adv. Mater. 14, 043501 (2013).D. J. Late, Y.-K. Huang, B. Liu, J. Acharya, S. N. Shirodkar, J. Luo, A. Yan, D. Charles, U. V. Waghmare, V. P. Dravid, and C. N. R. Rao, ACS Nano 7, 4879 (2013). Y. Li, H. Wang, L. Xie, Y. Liang, G. Hong, and H. Dai, J. Am. Chem. Soc. 133, 7296 (2011). M. Chhowalla, H. S. Shin, G. Eda, L.-J. Li, K. P. Loh, and H. Zhang, Nat. Chem. 5, 263 (2013).], also allows for superior electrostatic modulation of the carrier density, a feature that is necessary for continued nanoscale transistor scaling.

Yin et al [Xiaobo Yin, Ziliang Ye, Daniel A. Chenet, Yu Ye, Kevin O'Brien, James C. Hone, Xiang Zhang, 2 MAY 2014 VOL 344 SCIENCE] observed one-dimensional nonlinear optical edge states of a single atomic membrane of molybdenum disulfide (MoS_2), a transition metal dichalcogenide. The nonlinear optical responses that allows rapid and all-optical determination of the crystal orientations of the 2D material at a large scale. Mak et al [Kin Fai Mak1, Matthew Y. Sfeir2, Yang Wu1, Chun Hung Lui1, James A. Misewich2 and Tony F. Heinz1 and L.A. Falkovsky, Journal of Physics: Conference Series 129 (2008) 012004] have shown optical conductivity of graphene over the spectral range of 0.2 – 1.2 eV.

The rise in interest of antimonene (Sb) in photonics and optoelectronics is shown by its applications ranging from solar cells and light-emitting devices to touch screens, photo-detectors and ultrafast lasers. This is because the combination of its unique optical and electronic properties can be fully exploited in nano-photonics.

In this paper, we explored the electronic, and optical properties of antimonene (Sb). The present report is organized in four sections. Section 2 describes the methodology and theoretical formulation employed for the calculations. In section 3, the relevant density of states, refractive index and other properties of antimonene (Sb) is discussed. Discussion for optical properties of antimonene (Sb) explored in this section. Finally, short concluding remarks are presented in section 4.

COMPUTATIONAL DETAILS

Our first-principle calculations are based on density functional theory (DFT) as implemented in Vienna ab-initio Simulation Package (VASP) [1,2]and the standard Kohn-Sham equation [3] of the density functional theory in a plane-wave set with the projector- augmented wave (PAW) pseudopotentials to model the interactions between valence electrons and ionic cores.The exchange-correlation potentials approximated by Generalized Gradient Approximation (GGA) functional as parametrized by Perdew, Burke and Ernzerhof (PBE) [4] are used in our calculations. In the self-consistent field potential and total energy calculations is set to be (22×22×1) and (15×15×1) **k**-point sampling is used for Brillouin Zone (BZ) integration in **k**-space for the Alpha-Sb (α-Sb) and Beta-Sb (β-Sb) in two-dimensional (2D) system, respectively. The kinetic energy cutoff $\hbar^2|\mathbf{k}+\mathbf{G}|/2m$ for plane wave basic set is taken as 500 eV. All the atoms in the unit cell are fully relaxed until the force on each atom is below the 0.001 eV/Å and the energy convergence criteria for energy in self-consistent field (SCF) cycle is taken as 1×10^{-6} eV.The materials are periodic in XY-plane and separated by 20 Å along the z-direction to avoid the interaction between adjacent planes.

THEORETICAL METHODOLOGIES

The dielectric function can be written as $\boldsymbol{\varepsilon(\omega)= \varepsilon^1(\omega)+ i\varepsilon^2(\omega)}$, which used to describe the optical properties of materials.Here$\varepsilon^1(\omega)$ and $\varepsilon^2(\omega)$ are the real and imaginary part of complex dielectric function respectively.We have used DFT within the Random Phase Approximation (RPA) approximation [5].For calculating these components for α-Sb and β-SbAntimoneneMonolyaers, We have taken different polarizations of electric field with respect to the c axis (which is normal to the plane of 2D sheet) are taken into account. The frequency dependent dielectric matrix after the electronic ground state has been determined by using VASP [1-2]. The imaginary part is determined by a summation over empty states using the equation:

$$\varepsilon^2_{\alpha\beta}(\omega)=\frac{4\pi^2e^2}{\Omega}\lim_{q\to0}\frac{1}{q^2}\sum_{c,v,k}2w_k\delta(\varepsilon_{ck}-\varepsilon_{vk}-\omega)\left\langle u_{ck+e_\alpha q}\middle|u_{vk}\right\rangle\left\langle u_{ck+e_\beta q}\middle|u_{vk}\right\rangle^* \quad (1)$$

Herethe indices α and β are the Cartesian components, vectors e_α and e_β are the unit vectors along these directions. The indices *c* and *v* refer to conduction and valence band states respectively, and u_{ck} is the cell periodic port of the orbitals at the k-points k**.**

The real part of the dielectric tensorε^1 is obtained by the usual Kramers-Kronig relationship in the form [6-8]

$$\varepsilon^1_{\alpha\beta}(\omega)=1+\frac{2}{\pi}P\int_0^\infty\frac{\varepsilon^2_{\alpha\beta}(\omega')\omega'}{\omega'^2-\omega^2+i\eta}d\omega' \quad (2)$$

Where P denotes the principle value. The method is explained in detail in Ref. [5]If we assume orientation of the crystal surface perpendicular to the optical axis, the reflectivity R(ω) follows directivity from Fresnel's formula,

$$\boldsymbol{R}(\boldsymbol{\omega}) = \frac{[\boldsymbol{n}(\boldsymbol{\omega})-1]^2 + \boldsymbol{k}(\boldsymbol{\omega})^2}{[\boldsymbol{n}(\boldsymbol{\omega})+1]^2 + \boldsymbol{k}(\boldsymbol{\omega})^2} \tag{3}$$

Expression for the absorption coefficient I(ω), extinction coefficient k(ω), refractive index n(ω) and energy loss spectrum L(ω) are given as

$$I(\boldsymbol{\omega}) = \sqrt{2}\boldsymbol{\omega}\sqrt{|\boldsymbol{\varepsilon}(\boldsymbol{\omega})| - \boldsymbol{\varepsilon}^1(\boldsymbol{\omega})} \tag{4}$$

$$\boldsymbol{k}(\boldsymbol{\omega}) = \sqrt{\frac{|\boldsymbol{\varepsilon}(\boldsymbol{\omega})| - \boldsymbol{\varepsilon}^1(\boldsymbol{\omega})}{2}} \tag{5}$$

$$\boldsymbol{n}(\boldsymbol{\omega}) = \sqrt{\frac{|\boldsymbol{\varepsilon}(\boldsymbol{\omega})| + \boldsymbol{\varepsilon}^1(\boldsymbol{\omega})}{2}} \tag{6}$$

$$L(\omega) = \frac{\boldsymbol{\varepsilon}^2(\boldsymbol{\omega})}{\boldsymbol{\varepsilon}^2(\boldsymbol{\omega})^2 + \boldsymbol{\varepsilon}^1(\boldsymbol{\omega})^2} \tag{7}$$

$$\sigma(\omega) = \sigma_1(\omega) + i\ \sigma_2(\omega) = -i\frac{\omega}{4\pi}\left[\varepsilon(\omega) - 1\right] \tag{8}$$

Here $|\boldsymbol{\varepsilon}(\boldsymbol{\omega})| = \sqrt{\boldsymbol{\varepsilon}^1(\boldsymbol{\omega})^2 + \boldsymbol{\varepsilon}^2(\boldsymbol{\omega})^2}$ is it's the relative dielectric constant.

RESULTS AND DISCUSSION

A. Electronic density of states

We performed our calculation by adopted the indirect band gaps of both phases α-Sb and β-Sb are ≈0.28 eV and ≈0.78 eV of antimonene monolayers respectively [9]. The total density of states (TDOS) and partial density of states (PDOS) for α-Sb and β-Sb phases are shown in Fig 1. There are three sub-bands in the whole calculated energy range. For α-Sb and β-Sb, it is found that the lower valence bands between -11.20 eV and -9.59 eV are essentially dominant by *Sb-5s* states and shows hybridization with *Sb-4d*, *Sb-5s* and *Sb-5p* states. The contribution of Sb-5p states near the Fermi-level is more dominant as compare to *Sb-5s* and *Sb-4d* states in both phases (α-Sb and β-Sb). For β-Sbmonolayer, we found that the lower valence bands between -8.98 eV and -6.50 eV are essentially dominant by *Sb-5s* states and this is also shows hybridization with *Sb-5s*, *Sb-5p* and *Sb-4d* states. In case of *β-Sb*, the contribution in total DOS of *Sb-5p* is more near the Fermi-level that mean *Sb-5p* states are dominant as compare to *Sb-4p* states.

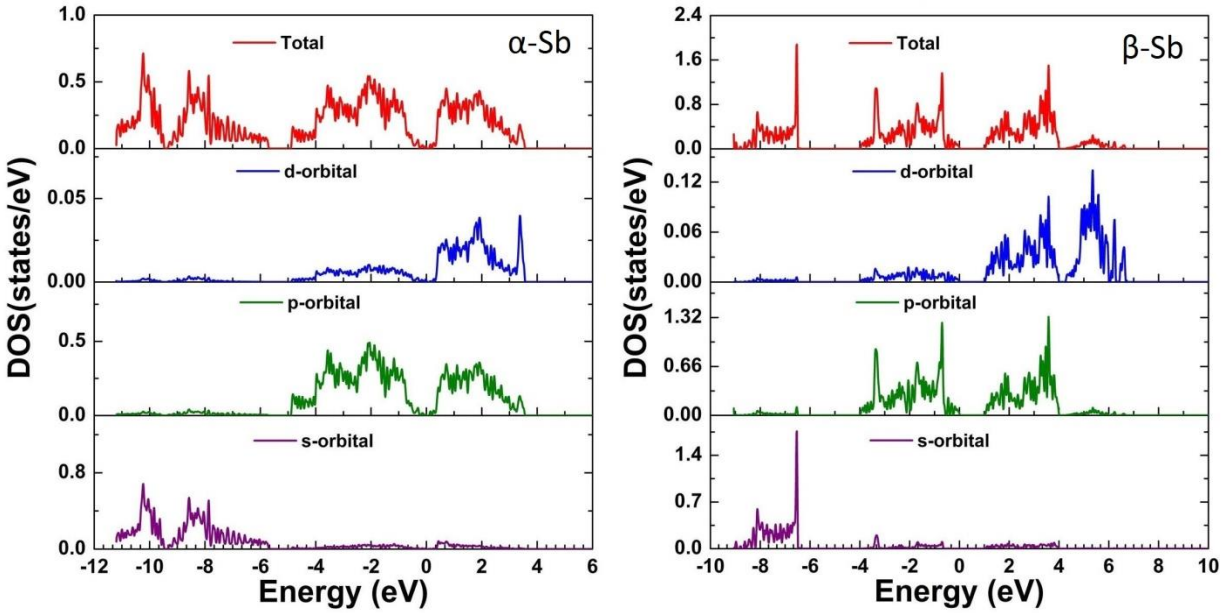

Figure 1 The total and partial density of states ofα-Sb and β-Sb monolayers

B. Optical properties

In our calculation we computed, the optical properties like dielectric function, energy loss spectrum, absorption coefficient, reflectivity, refractive index and extinction coefficient of graphene-like α-Sb and β-Sb compounds. The intra-band and inter-band contribution of the transitions can be involved by the imaginary part of complex dielectric function that would be obtained by equation-(1). The real and imaginary parts of the complex dielectric function $\varepsilon(\omega)$are displayed in Fig.2. In the real dielectric function $\varepsilon^1(\omega)$ gives information about the electronic polarizability of the material.

Antimonene Allotropes	Refractive index	Reflectivity (%)	Plasmonic energy(eV)
α-Sb	1.98	52	9.35
β-Sb	1.53	43	9.40

The static dielectric constant with the zero frequency limit is obtained as $\varepsilon^1(0)=3.95$ and $\varepsilon^1(0)=4.25$ for α-Sb and β-Sb respectively. In the real part of dielectric function, one negative value for the range 4.53 eV, 9.06 eV and 5.58 eV, 8.82 eV for both phase α-Sb and β-Sb. This indicates that the two phases of α-Sb and β-Sb monolayers shows a metallic behavior in this frequency zone. Our results shows the good agreement with 3-D material “quaternary arsenide oxides YZnAsO and LaZnAsO” by SHI Yi-ming et.al [10,11]

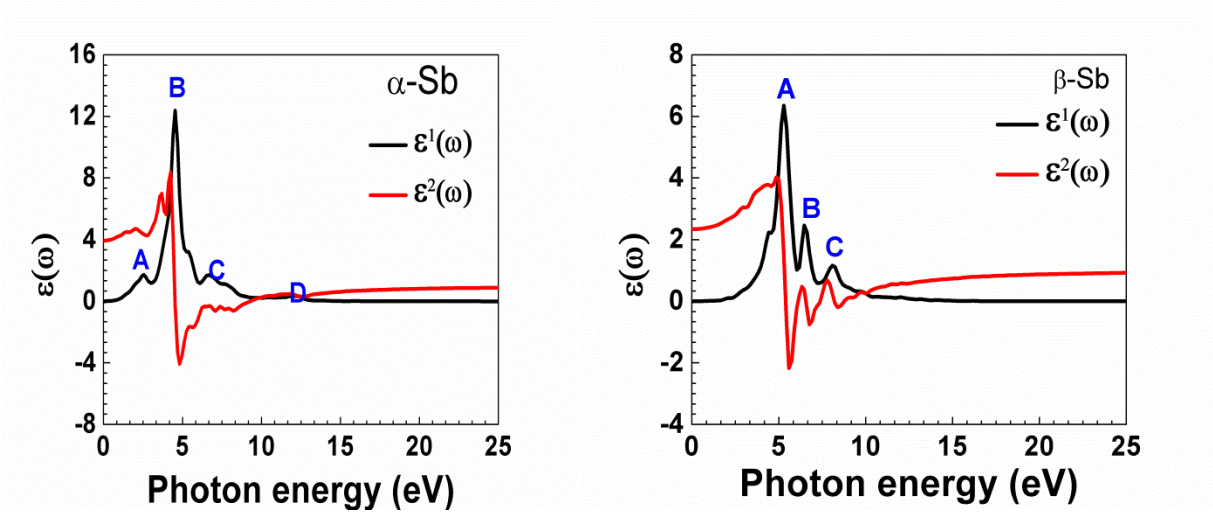

Figure 2 The real and imaginary part of complex dielectric function of α-Sb and β-Sbmonolayers.

In the imaginary part of dielectric function $\varepsilon^2(\omega)$, there are several peaks, which are identified by the symbols A (1.71 at 3.40 eV), B (12.39 at 4.53 eV), C (1.66 at 6.52 eV) and D (0.35 at 12.20 eV) for α-Sb. And for β-Sb there are mainly three peaks only, which identified by the symbols A (6.35 at 5.29 eV), B (2.46 at 6.47 eV) and third peak C (1.11 at 8.23 eV). The recently Wang et.al [9,10] have given the fundamental gaps are 0.28 eV and 0.76eV for two stable phases of antimonene α-Sb and β-Sb. The minimum energy of the dielectric function occurs at $E_0=0.28$ *eV* for α-Sb monolayer and $E_0=0.76$*eV* for β-Sb monolayer, which corresponds to the fundamental gaps at equilibrium. It is well known that materials with band gaps below the 1.55 eV work well in the infrared (IR) region of the spectrum. Therefore α-Sb and β-Sb both phases will work in the IR-region as an optical material.

All these three peaks A, B, C in imaginary part of dielectric function (at 2.53 eV, 4.53 eV and 6.52 eV) is mainly due to the electronic transitions from *Sb-4d* in the valence band to *Sb-5p* in the conduction band or it may be possible, the electronic transition from Sb-5p in the valence band to *Sb-4d* in the conduction band. At the next D peak (at 12.18 eV) occurs due to the transition from *Sb-5s* in the valence band to *Sb-4d* or *Sb-5p* in the conduction band for *α-Sb*. In the case of β-Sb, there are two peaks in imaginary part of dielectric function A, B (at 5.29 eV and 6.47 eV) is mainly due to the electronic transitions from Sb-4d in the valence band to Sb-5p in the conduction band or it may be possible, the electronic transition from Sb-5p in the valence band to Sb-4d in the conduction band. And the next D peak (at 8.23 eV) occurs due to the transition from Sb-5s in the valence band to Sb-4d or Sb-5p in the conduction band.

The refractive index *n(ω)* and extinction coefficient *K(ω)* are represented in Fig.3. The static refractive index *n(0),* which implies the important quantity has the values 1.98 and 1.53 of α-Sb and β-Sb phases respectively and it is approximately same result by Saha, Sonali et.al [12] . The maximum refractive index occurs 3.12 at 4.25 eV and 2.22 at 4.99 eV for α-Sb and β-Sb

monolayer respectively. From *K(ω)* the local maxima of the extinction coefficient *K(ω)* correspond to the zero of $\varepsilon^1(\omega) \approx 4.53$ eV for α-Sb and $\varepsilon^2(\omega) \approx 5.59$ eV for β-Sb monolayers.The refractive index *n(ω)* increases with energy in both the IR and Visibleregion. The spectrum curve of refractive index *n(ω)* and extinction coefficient *K(ω)* is rapidly decrease with increasing photon energy in UV region and it will becomes constant after 16 eV in both phases α-Sb and β-Sb.

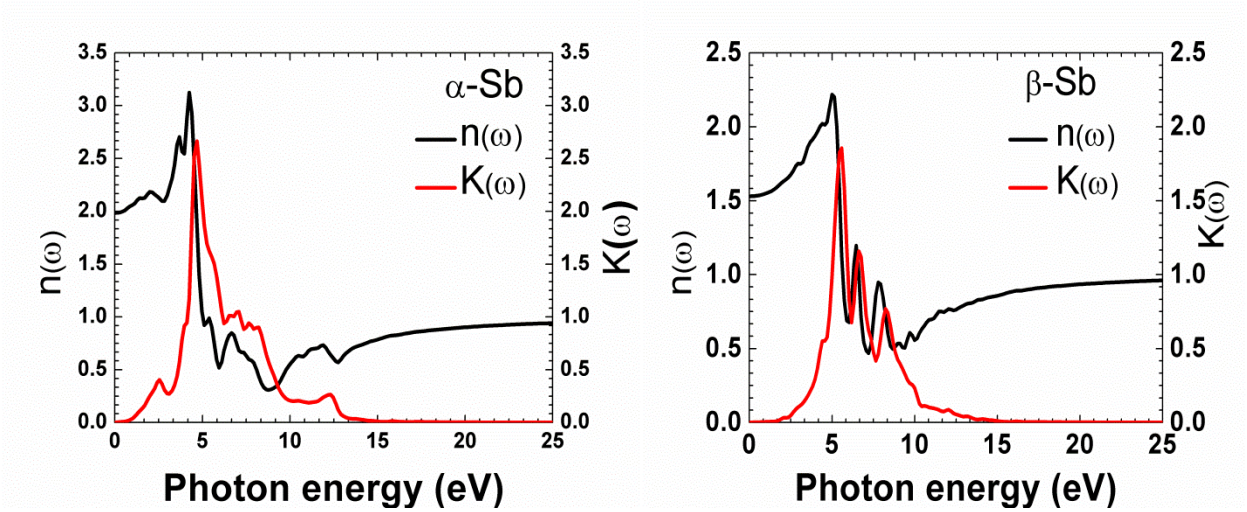

Figure 3 The refractive index *n(ω)* and extinction coefficient *K(ω)* ofα-Sb and β-Sb of monolayer.

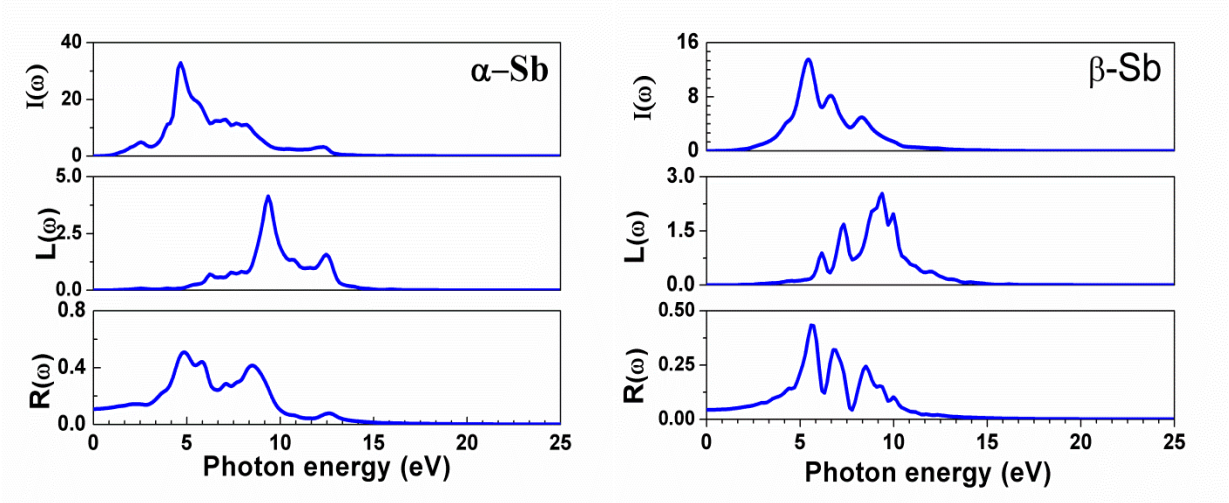

Figure 4 Therefractivity R(ω), energy loss spectrum L(ω) and absorption coefficient *I(ω)* ofα-Sb and β-Sb monolayers.

The absorption coefficient *I(ω)* of two phases α-Sb and β-Sb is shown in fig 4. Absorption coefficient is a percentage that tells the decay of light intensity spreads in unit distance in the medium. The calculated absorption coefficient for both phase α-Sb and β-Sb is almost zero when

the energy is below 0.28 eV and 0.59 eV respectively. When the photon energy is larger than the value of the absorption coefficient will increase, which corresponds to the reported indirect band gaps ≈ 0.28eV and 0.78eV for α-Sb and β-Sb respectively. There are many peaks within the energy range studied and peaks structure can be explain by the inter-band transitions using partial and total density of state. The absorption spectrum starts from about 0.28 eV and 0.57 eVα-Sb and β-Sb, after which the intensity varies with the increase in photon energy, and reaches a maximum value of 30.99×10^5 at 4.53 eV. There is no electronic transition in the low energy range E < 0.28 eV and E < 0.57 eV for α-Sb and β-Sbbecause the energy of the photon is lower than the band gap of the material. The first peak in the absorption spectrum occurs at 2.55 eV and other peaks occur at 4.53 eV, 7.08 eV, 8.22 eV and 12.18 eV for α-Sb and in case of β-Sb, the first peak in the absorption spectrum occurs at 5.29 eV and others peaks occurs at 6.46 eV and 7.93 eV.

We are able to optimize the different properties of material by the contribution of energy loss spectrum *L(ω)*. There are several ways for excitation of electrons in medium other than absorption of photon. In the solid when the fast electron travelling in the medium it may loss some energy which is represented by *L(ω)* and excites the electrons of solid. The intra and inter-band transmissions, Plasmon excitations can be identified by analyzing *L(ω)* which is related to the dielectric function by equation (7). The highest peaks on *L(ω)*, spectra represents the characteristics associated with the plasma resonance and the corresponding frequency is known as plasma frequency[13]. The peaks of *L(ω)* also correspond to the trailing edges in the reflection spectra[11]. There are two peaks associated in α-Sb 9.35eV and 12.46eV.For β-Sb, there are three peaks seen in L(ω) which is 6.17eV, 7.35eV and 9.40eV corresponding to the abrupt reduction of reflectivity R(ω). In our calculation Plasmon frequency of α-Sb and β-Sb are approximately same where the electric field is perpendicular to the plane. It is notice that, there are several peaks in reflectivity curve in the calculated photon energies up to 16eV for two phases of antimonene which is α-Sb and β-Sb it will becomes constant. The maximum reflectivity reaches the values 52% and 43% for α-Sb and β-Sb respectively and maximum peak occurs at 4.82eV and 5.58eV for α-Sb and β-Sb.

CONCLUSIONS

As shown in results, density functional theory(DFT) within random phase approximation (RPA) calculation are performed on 2D antimonene monolayers atomic layer as mention in Wang et.al [9]α-Sb and β-Sb monolayer are stable so we did calculations on optical properties likes dielectric function, absorption spectrum, reflectivity, refractive index and energy loss spectrum of two phases α-Sb and β-Sbmonolayers with single later has been calculated for light polarization perpendicular to the plane of antimonene sheet. In the both phase, Plasmon peak are found at 9.35eV and 9.40eV for α-Sb and β-Sb. The calculated static refractive index and reflectivity are found 1.98, 1.53 and 52%, 43% for α-Sb and β-Sb respectively. Our calculated

results suggest further experimental investigations in this regard which could lead to application of α-Sb and β-Sb in field of photonics where absorption in visible region is required and it may be provides a new material that has possibility to be applied in microelectronic, optoelectronics devises and solar cell.

REFERENCES

1. G. Kresse and J. Furthmüller, Phys. Rev. B, 54, 11169-11186 (1996)
2. G. Kresse and D. Joubert, Phys. Rev. B, 59, 1758-1775 (1999)
3. W. Kohn and L. J. Sham, Phys. Rev. A, 140 1133-1138 (1965)
4. J. P. Perdew, K. Burke and M. Ernzerhof, Phys. Rev. Lett., 77, 3865-3868 (1996)
5. M. Gajdoš, K. Hummer and G. Kresse, Phy. Rev. B, 73, 045112 (2006)
6. D. C. Ambrosch and J. O. Sofo, Comput. Phys. Commun. 175, 1 (2006)
7. M. Fox, Optical Properties of Solids, New York: Oxford University Press, (2001)
8. F. Wooten, Optical Properties of Solids, New York: Acadmic Press, (1972)
9. G. Wang, R. Pandey and S. P. Karna, ACS Appl. Mater. Interfaces, 7, 11490−11496 (2015)
10. Yi-ming, S. H. I., and Y. E. Shao-long. *The Chinese Journal of Nonferrous Metals* 21.6 (2015).
11. Sharma, Jyoti Dhar, et al. *Journal of Physics: Conference Series*. Vol. 472. No. 1. IOP Publishing, 2013.
12. Saha, Sonali, T. P. Sinha, and Abhijit Mookerjee. *Physical Review B* 62.13 (2000): 8828.
13. Lashgari, H., et al. *Solid State Communications* 195 (2014): 61-69.